

Microfluidic Solution-Processed Organic and Perovskite Nanowires Fabricated for Field-Effect Transistors and Photodetectors

Ping-An Chen¹, Jing Guo¹, Mehdi Nouri², Quanyang Tao³, Zhiwei Li³, Qianyuan Li³,
Lulu Du⁴, Huajie Chen⁴, Zaizai Dong^{5,6}, Lingqian Chang^{5,6*}, Yuan Liu³, Lei Liao¹,
Yuanyuan Hu^{1*}

¹Key Laboratory for Micro/Nano Optoelectronic Devices of Ministry of Education and Hunan Provincial Key Laboratory of Low-Dimensional Structural Physics and Devices, School of Physics and Electronics, Hunan University, Changsha 410082, China

²Department of Biomedical Engineering, University of North Texas, Denton, TX, 76207, US

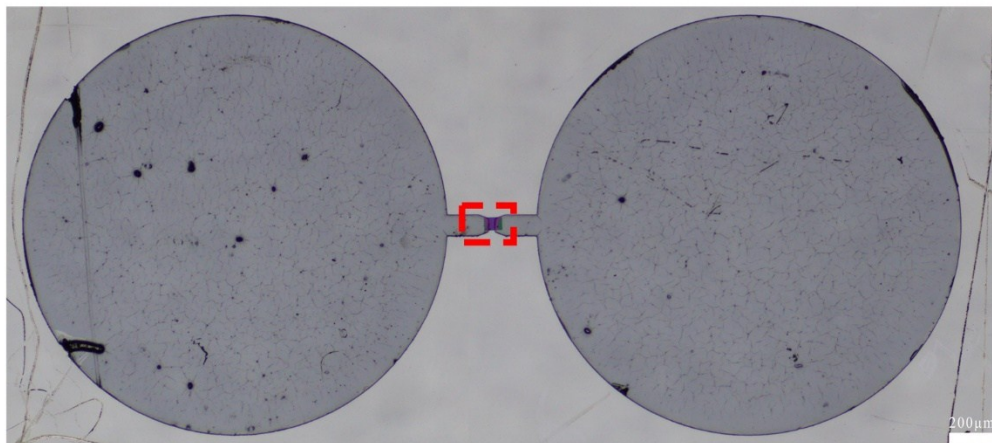
³Hunan Key Laboratory of Two-Dimensional Materials and State Key Laboratory for Chemo/Biosensing and Chemometrics, School of Physics and Electronics, Hunan University, Changsha 410082, China

⁴Key Laboratory of Environmentally Friendly Chemistry and Applications of Ministry of Education, College of Chemistry, Xiangtan University, Xiangtan 411105, China

⁵School of Biological Science and Medical Engineering, Beihang University, Beijing 100083, China

⁶Institute of Nanotechnology for Single Cell Analysis (INSCA), Beijing Advanced Innovation Center for Biomedical Engineering, Beihang University, Beijing 100083, China

(a)



(b)

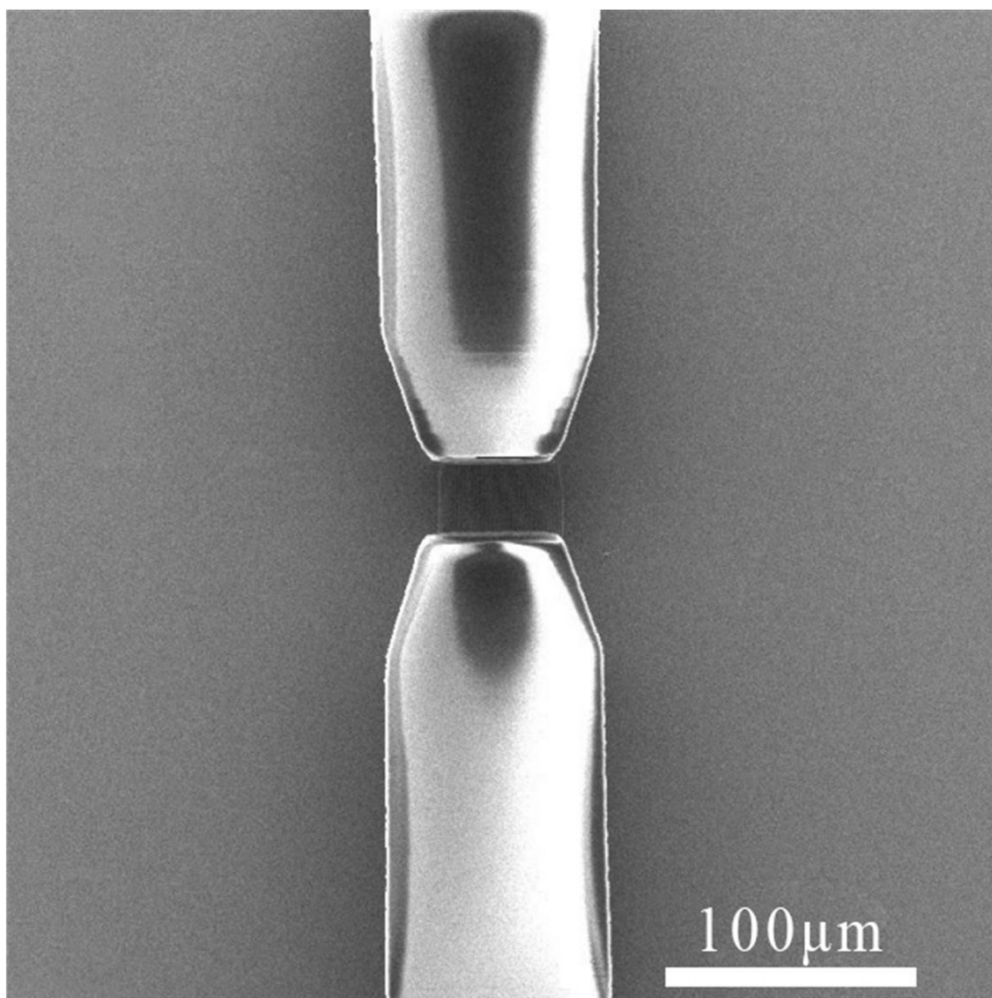


Figure S1. (a) Optical microscope image of nanowires template. (b) SEM image of nanowires template.

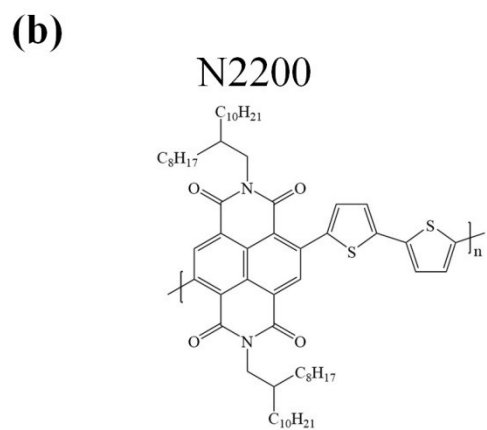
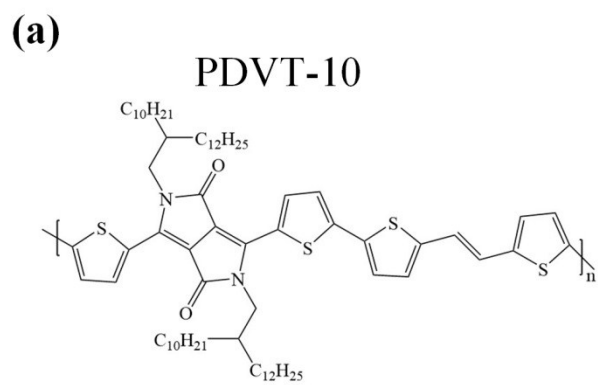


Figure S2. The molecule structures of (a) PDVT-10 and (b) N2200.

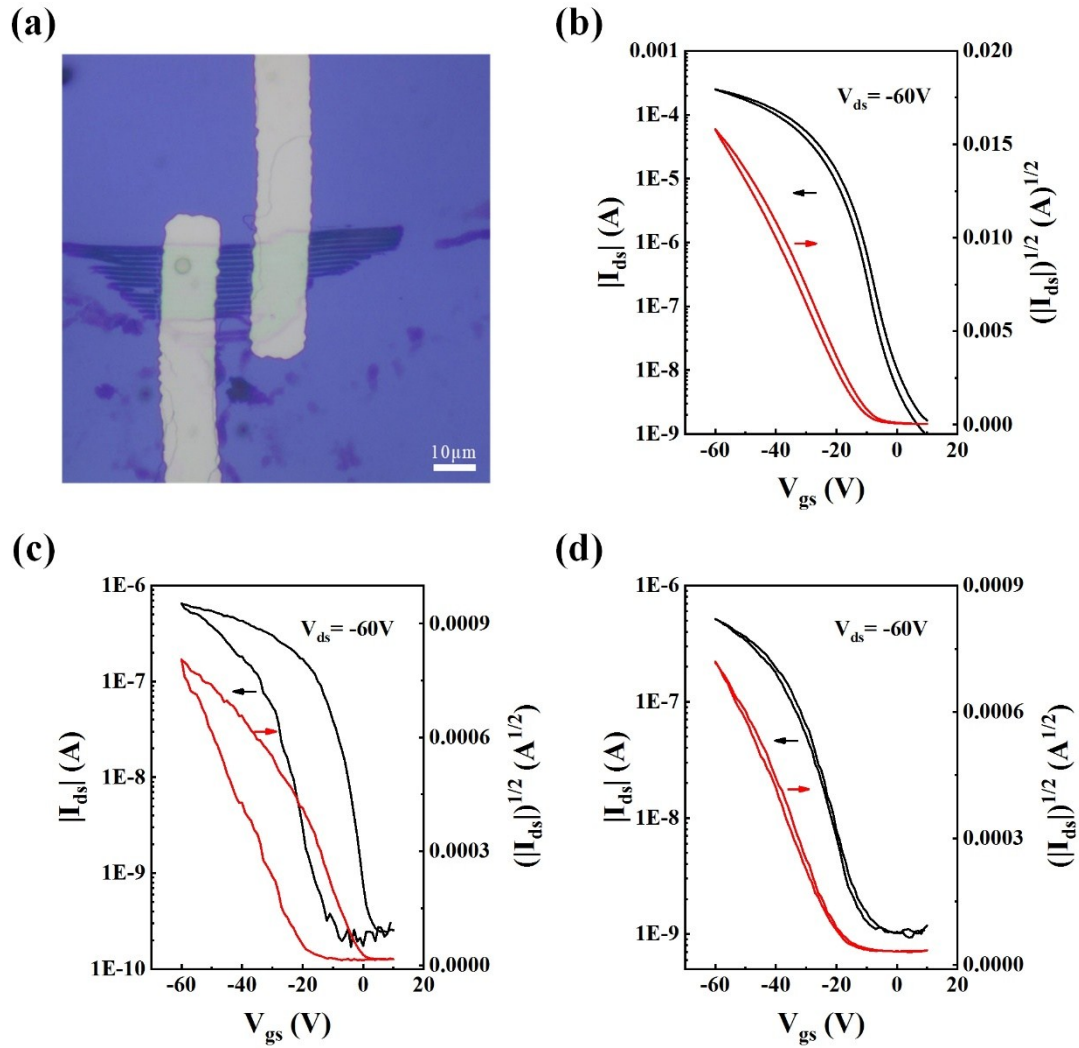
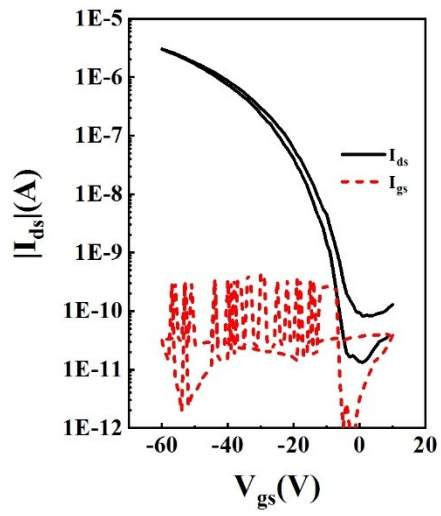


Figure S3. (a) Device appearance and channel region. (b) Transfer characteristics (I_{ds} - V_{gs}) of PDVT-10 thin-film transistors (BGTC) with $L = 30 \mu\text{m}$ and $W = 1000 \mu\text{m}$, exhibiting a hole mobility of $0.32 \text{ cm}^2\text{V}^{-1}\text{s}^{-1}$ at $V_{ds} = -60 \text{ V}$. (c) Transfer characteristics (I_{ds} - V_{gs}) of PDVT-10 nanowire transistors (BGBC) with $L = 20 \mu\text{m}$ and $W = 9 \mu\text{m}$, exhibiting a hole mobility of $0.06 \text{ cm}^2\text{V}^{-1}\text{s}^{-1}$ at $V_{ds} = -60 \text{ V}$. (d) Transfer characteristics (I_{ds} - V_{gs}) of PDVT-10 nanowire transistors (TGBC) with $L = 20 \mu\text{m}$ and $W = 6.3 \mu\text{m}$, exhibiting a hole mobility of $0.1 \text{ cm}^2\text{V}^{-1}\text{s}^{-1}$ at $V_{ds} = -60 \text{ V}$.

(a)



(b)

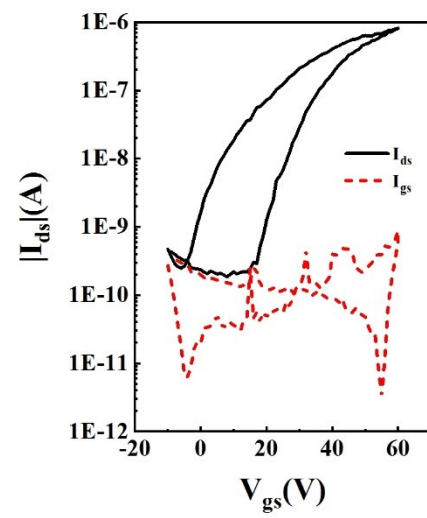


Figure S4. Transfer characteristics of (a) PDVT-10 nanowire transistor (BGTC) and (b) N2200 nanowire transistors (BGBC) at $|V_{ds}|=60$ V.

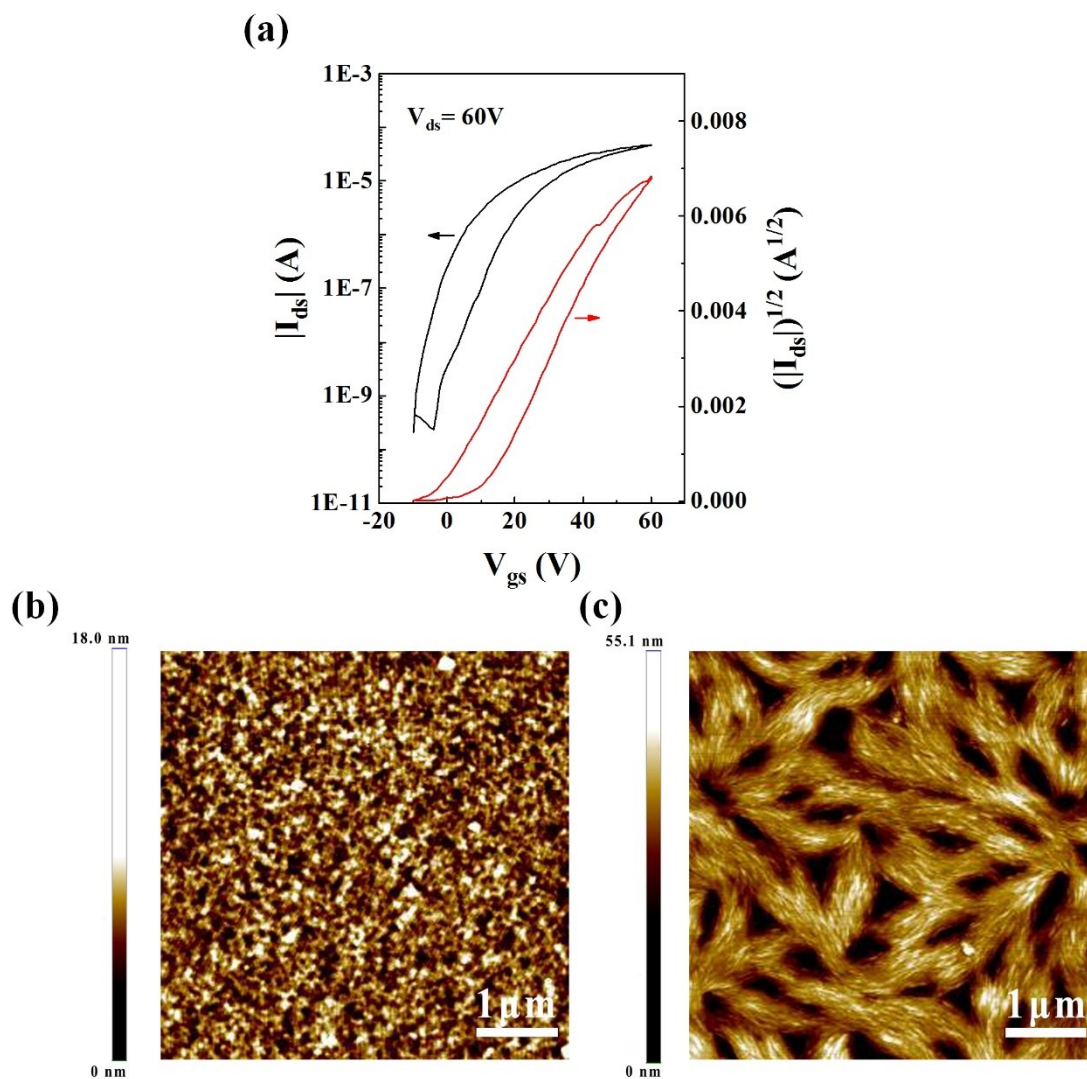


Figure S5. (a) Transfer characteristics (I_{ds} - V_{gs}) of a typical N2200 thin-film transistors (BGBC) with $L = 20 \mu\text{m}$ and $W = 1000 \mu\text{m}$, exhibiting a hole mobility of $0.02 \text{ cm}^2\text{V}^{-1}\text{s}^{-1}$ at $V_{ds} = 60 \text{ V}$. AFM images of (b) PDVT-10 and (c) N2200 thin-film on OTS-modified Si/SiO₂ substrates, respectively.

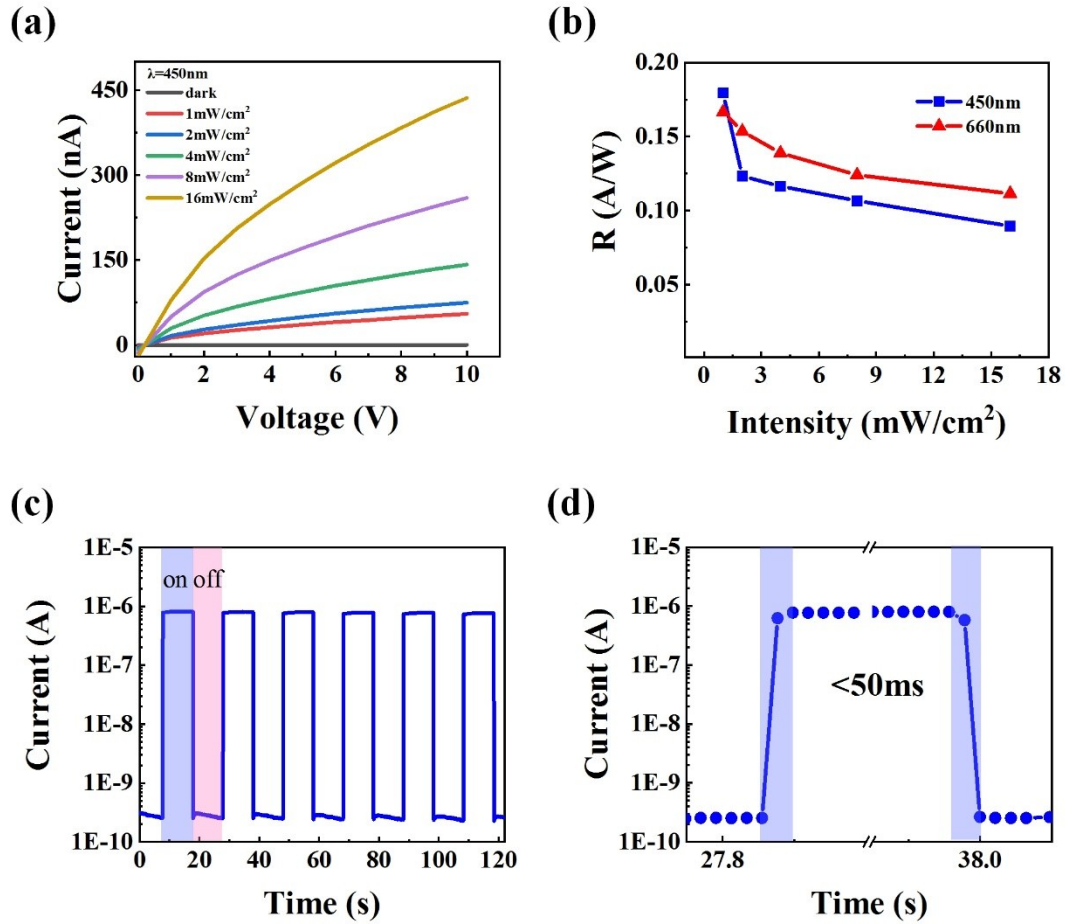


Figure S6. (a) I - V curves of the pristine MAPbI₃ thin-film under illumination of 450 nm with a power density varying from 0 to 16 mW/cm². (b) Responsivity as a function of the light power density for pristine MAPbI₃ film photodetectors at 5 V and wavelengths of 450 nm and 660 nm. (c) The time-dependent photocurrent measurement of MAPbI₃ film photodetector under illumination of 450 nm at 5 V, and (d) the rise and fall times response.

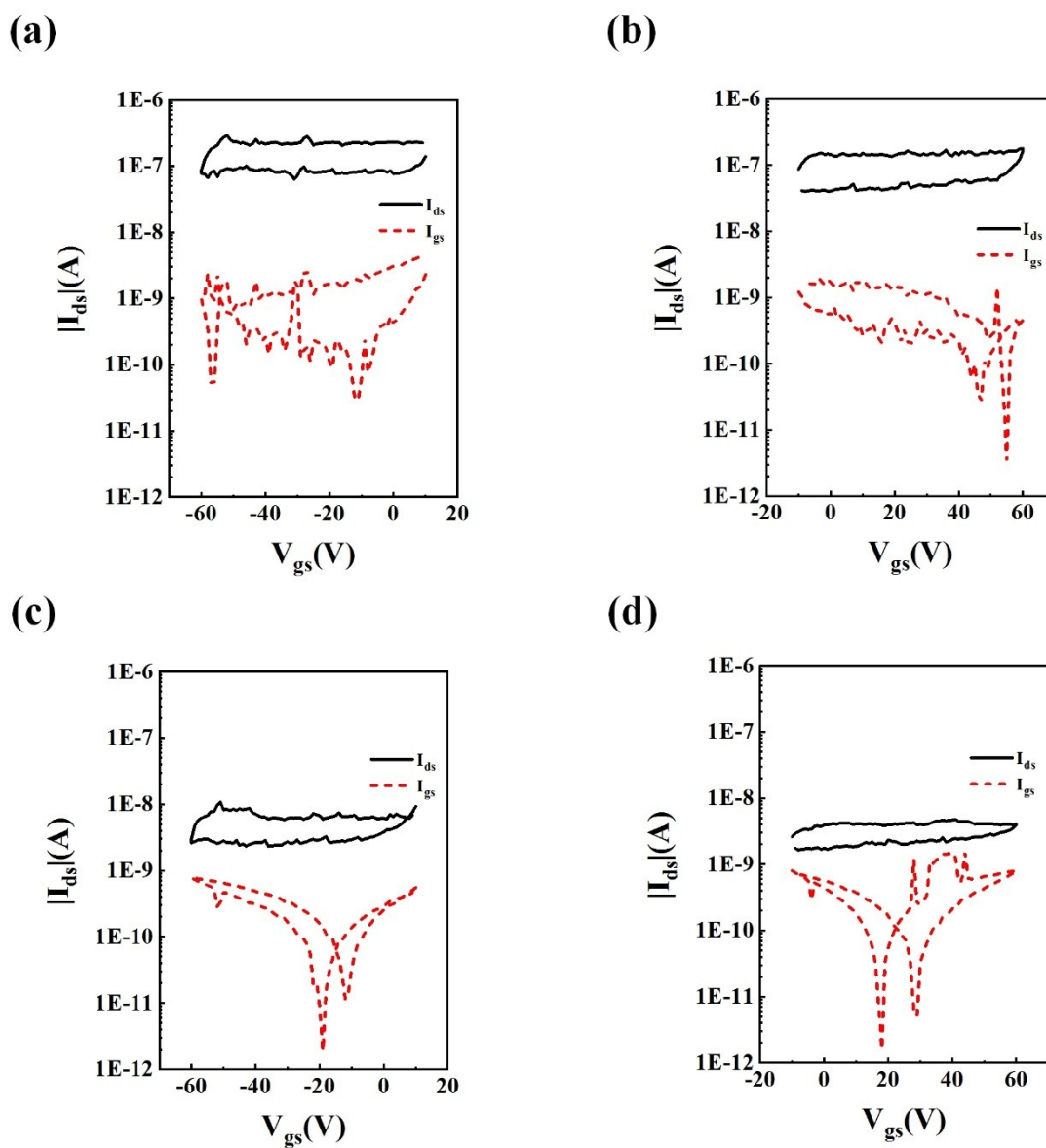


Figure S7. Transfer characteristics (I_{ds} - V_{gs}) of MAPbI₃ thin-film transistors under $|V_{ds}|=60$ V (a) p-type and (b) n-type. Transfer characteristics (I_{ds} - V_{gs}) of MAPbI₃ nanowire transistors under $|V_{ds}|=60$ V (a) p-type and (b) n-type.

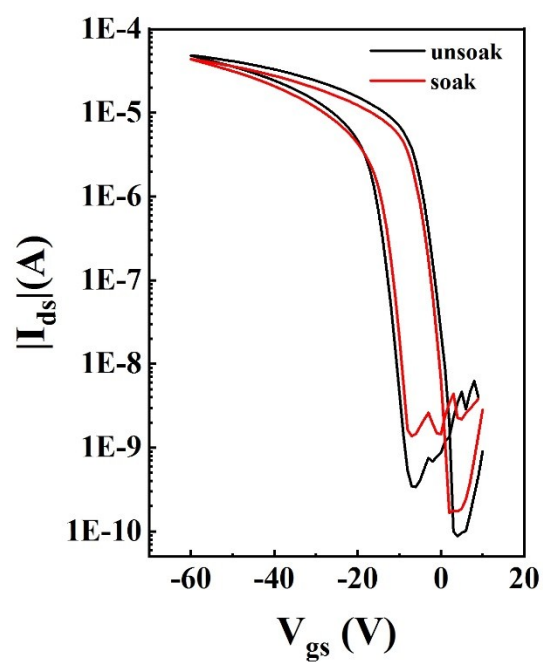
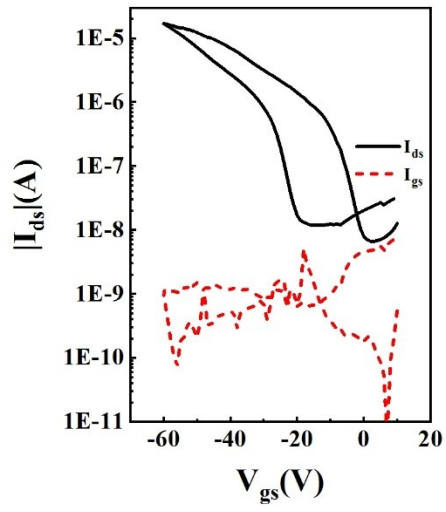


Figure S8. Transfer characteristics (I_{ds} - V_{gs}) of the thin-film (PDVT-10) before and after the immerse.

(a)



(b)

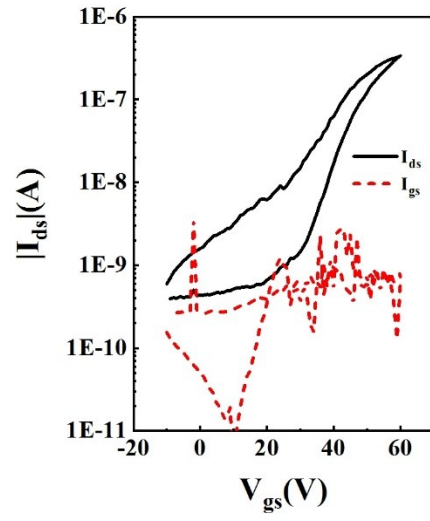


Figure S9. Transfer characteristics of (a) MAPbI₃/PDVT-10 and (b) MAPbI₃/N2200 nanowire heterojunction transistors at $|V_{ds}|=60$ V.

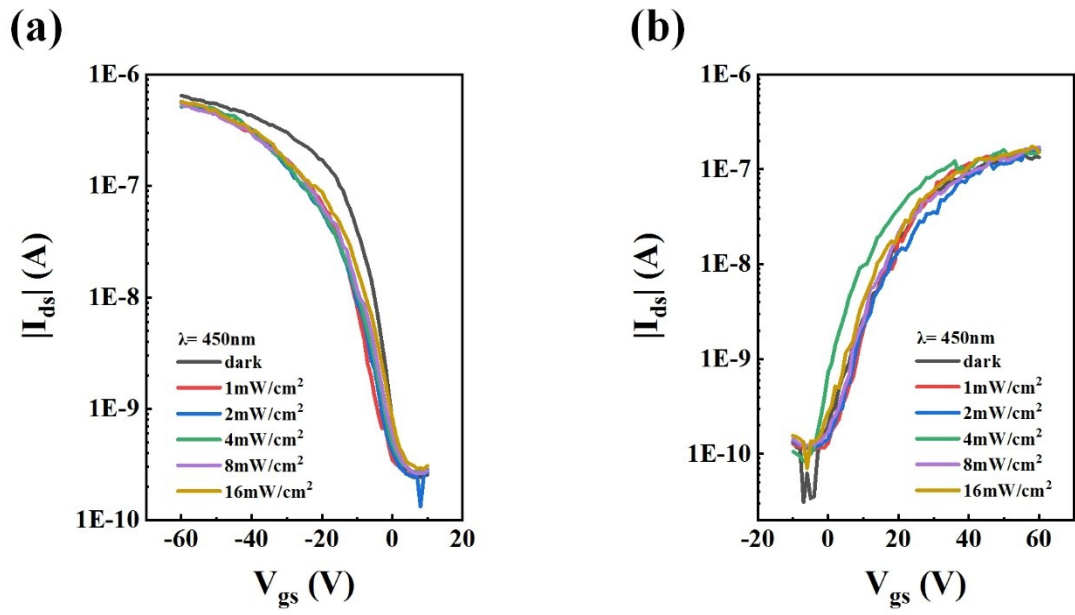


Figure S10. Transfer characteristics (I_{ds} - V_{gs}) of the (a) PDVT-10 and (b) N2200 nanowire transistors under light of 450 nm with power intensity varying from 0 to 16 mW/cm².

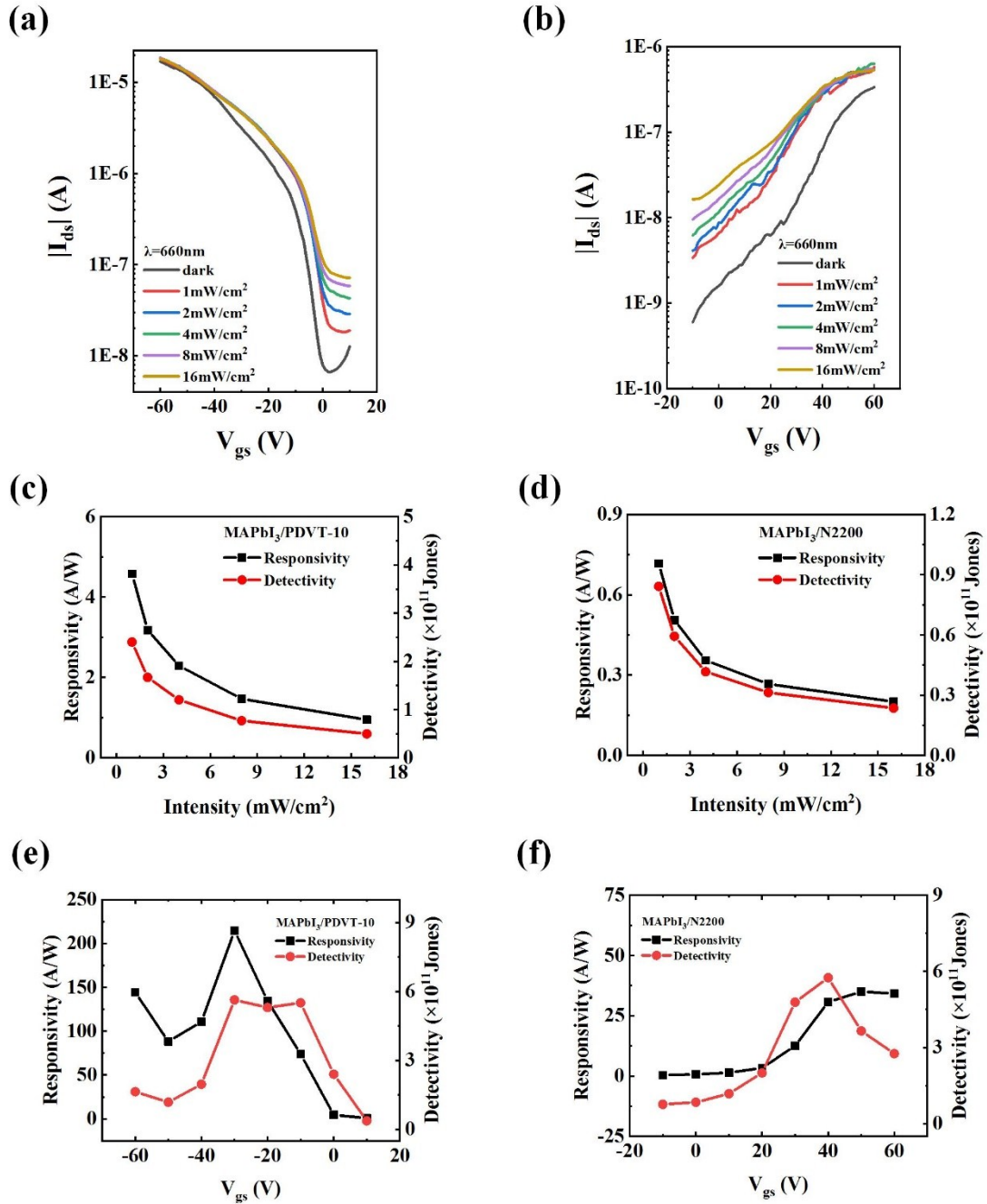


Figure S11. Photo response of MAPbI₃/OSC nanowire heterojunction transistors. Transfer characteristics (I_{ds} - V_{gs}) of the (a) MAPbI₃/PDVT-10 and (b) MAPbI₃/N2200 nanowire heterojunction transistors under illumination of 660 nm light. Photoresponsivity (R) and detectivity (D^*) characteristics of (c) MAPbI₃/PDVT-10 and (d) MAPbI₃/N2200 nanowire heterojunction transistors at $V_{gs} = 0$ V under illumination of 660 nm light. The dependences of R and D^* on V_{gs} under illumination of 660 nm light for (e) MAPbI₃/PDVT-10 and (f) MAPbI₃/N2200 nanowire heterojunction transistors.

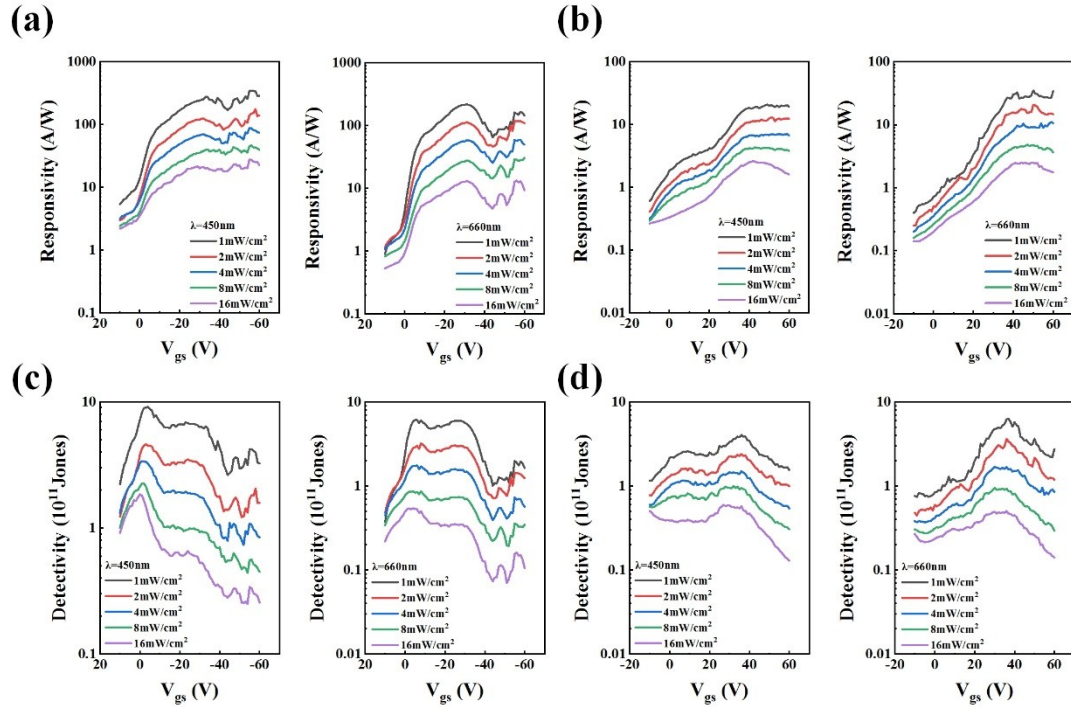


Figure S12. The dependences of R characteristics on V_{gs} under illumination of 450 nm or 660 nm light for (a) MAPbI₃/PDVT-10, (b) MAPbI₃/N2200 nanowire heterojunction phototransistors, respectively. The dependences of D^* on V_{gs} under illumination of 450 nm or 660 nm light for (c) MAPbI₃/PDVT-10, (d) MAPbI₃/N2200 nanowire heterojunction phototransistors, respectively.